

Connectomic Underpinnings of Working Memory Deficits in Schizophrenia: Evidence From a replication fMRI study

Jie Yang¹, Weidan Pu^{2,3}, Guowei Wu¹, Eric Chen⁴, Edwin Lee⁴, Zhening Liu^{*,1}, and Lena Palaniyappan^{1,5-7}

¹Institute of Mental Health, Second Xiangya Hospital, Central South University, Changsha, PR China; ²Medical Psychological Center, the Second Xiangya Hospital, Central South University, Changsha, P.R. China; ³Medical Psychological Institute of Central South University, Changsha, P.R. China; ⁴Department of Psychiatry, The University of Hong Kong, Pok Fu Lam, Hong Kong; ⁵Department of Psychiatry, University of Western Ontario, London, ON, Canada; ⁶Robarts Research Institute, University of Western Ontario, London, ON, Canada; ⁷Lawson Health Research Institute, London, ON, Canada

*To whom correspondence should be addressed; Zhening Liu, Institute of Mental Health, the Second Xiangya Hospital, Central South University, Changsha, China. tel: 86-0731-85296818, fax: 86-0731-85533525, e-mail: Zhening.liu@csu.edu.cn

Background: Working memory (WM) deficit is a key feature of schizophrenia that relates to a generalized neural inefficiency of extensive brain areas. To date, it remains unknown how these distributed regions are systemically organized at the connectome level and how the disruption of such organization brings about the WM impairment seen in schizophrenia. **Methods:** We used graph theory to examine the neural efficiency of the functional connectome in different granularity in 155 patients with schizophrenia and 96 healthy controls during a WM task. These analyses were repeated in another independent dataset (81 patients and 54 controls). Linear regression analysis was used to test associations of altered graph properties, clinical symptoms, and WM accuracy in patients. A machine-learning approach was adopted to study the ability of multivariate connectome features from one dataset to discriminate patients from controls in the second dataset. **Results:** Small-worldness of the whole-brain connectome was significantly increased in schizophrenia during the WM task; this increase is related to better (though subpar) WM accuracy in patients with more severe negative symptom burden. There was a shift in the degree distribution to a more homogeneous form in patients. The machine-learning approach classified a new set of patients from controls with 84.3% true-positivity rate for schizophrenia and 71.6% overall accuracy. **Conclusions:** We demonstrate a putative mechanistic link between connectome topology, hub redistribution, and impaired *n*-back performance in schizophrenia. The task-dependent modulation of the connectome relates to, but remains inefficient in, improving the performance above par in the presence of severe negative symptoms.

Key words: schizophrenia/functional connectome/neural efficiency/graph theory/working memory

Introduction

Neurocognitive dysfunction is one of the core features of schizophrenia.^{1,2} Of the various neurocognitive deficits in schizophrenia, working memory (WM) deficit, the failure to represent, maintain, and update information in a short period of time, is a key feature that determines the degree of successful functional recovery.³ WM deficits persist despite treatment, resulting in a lifelong illness burden⁴ that may also contribute to recurrent relapses⁵ and the burden of negative symptoms.⁶⁻⁹ Negative symptoms have been evidenced as the symptom dimension most strongly associated with neurocognitive function¹⁰ and often mediating the relationship between neurocognition and functional outcome.^{11,12}

A large body of research probing the neural mechanism of WM dysfunction in schizophrenia has revealed that patients have functional hyperconnectivity within the default-mode network (DMN),^{13,14} hypoconnectivity within the frontoparietal network (FPN),^{15,16} and reduced functional interaction among large-scale networks including the DMN, FPN, cingulo-opercular or salience network.^{17,18} Highly connected core hubs show reduced overall functional connectivity but peripheral hubs that are typically less connected in healthy subjects exhibit higher functional connectivity during *n*-back task.¹⁹ In addition, patients also show a failure to deactivate DMN regions, but recruit (activate) other task-irrelevant regions to perform WM tasks.^{20,21} Taken together, these results suggest that a generalized neural inefficiency affecting extant cortical and subcortical areas with a redistribution of core hubs during WM performance in schizophrenia.²²

The employment of mathematical graph theory tools to functional neuroimaging data (functional topology) has provided an intuitive method to study the neural

efficiency at a whole-brain (connectome) level. Functional connectome studies have revealed that brain networks are organized in an efficient small-world manner (ie, a highly clustered/segregated neighborhood of brain regions, with occasional integrative long-distance connections) that confers high efficiency of information processing at relatively low connection cost.^{23,24} Such small-world-like organization of task-related networks predicts interindividual differences in WM capacity as well as within-subject variations in WM performance among healthy individuals.²⁵ In particular, increased integration instead of segregation when faced with task demands appears to confer an adaptive advantage to functional networks.²⁶ To date, it is unclear whether such an adaptive advantage toward neural efficiency is impaired in patients with schizophrenia when facing task demands.

Among patients with schizophrenia, several studies related to electroencephalography (EEG), functional magnetic resonance image (fMRI), and magnetoencephalography (MEG) have identified a sub-optimal small-world configuration during WM performance when compared with healthy controls,^{26–29} but the results have been mixed.³⁰ While some groups noted reduced small-worldness due to reduced local clustering (desegregation),^{31,32} others have observed normal^{26,27} or increased segregation³³ as well as disintegration (increased path length³³). These conflicting results are likely due to the differences in imaging modality, task differences, variations in illness severity as well as the definition of nodes (eg, He et al restricted the network construction to a subset of task-related networks) and edges in the connectome. In particular, all of the previous fMRI studies (synthesized by Kambeitz et al³⁰) employed unweighted binary matrices with proportional edge-density thresholds to construct the functional connectome where edges are treated as present or absent arbitrarily. While studying dysconnectivity disorders such as schizophrenia, wherein systematic differences exist in the overall strength of connectivity when compared with healthy controls, the binarization approach results in noisy and spurious edges with low connectivity strength in the patient group. This produces an apparent (but inconsistent) group difference in topological metrics, with a shift toward randomness in the group with weaker overall connectivity that can be avoided when using a weighted matrix approach.^{34,35}

The aim of the current study was to investigate how functional connectome topology is affected during WM performance in schizophrenia. To this end, we constructed weighted networks from 2-back WM fMRI data to test the hypothesis that aberrant small-world topology and redistribution of functional hubs occur during the WM task in schizophrenia. We expected a higher burden of negative symptoms to be associated with more severe WM deficits, and this relationship is being influenced by altered small-world topology. We also tested if the topological indices from WM fMRI data carry sufficient

illness-specific information that can discriminate the patterns observed in a patient with schizophrenia from the patterns that come from healthy controls. To this end, we employed a Support Vector Machine (SVM) approach to discriminate patients from controls using the independent discovery and validation datasets of *n*-back fMRI. This allowed us to estimate the generalizability (ie, the degree to which the pathophysiological model in one group translates to a new group), an essential step for translational neuroimaging.³⁶

Methods

Participants

The study cohort comprised a principal dataset (Dataset 1) of 155 patients and 96 HCs and an independent replication dataset (Dataset 2) of 81 patients and 54 HCs. All participants were right-handed native Chinese speakers and they were provided written informed consent for the protocols approved by the Department of Psychiatry, the Second Xiangya Hospital of Central South University, China. Detailed descriptions of all participants are presented in the [supplementary material S1](#).

MRI Data Acquisition and Preprocessing

Dataset 1 and dataset 2 were acquired on a Philips Achieva 3-T scanner and Siemens Allegra 3-T scanner, respectively. Scanning factors differed slightly across sites (detailed information is presented in [supplementary material S2](#)), and these differences were taken into account during preprocessing.

Data preprocessing was performed using the DPABI toolbox. Preprocessing included: discarded several images to reach magnetic saturation, slice timing correction, motion realignment, spatial normalization to Montreal Neurologic Institute space, and smoothing. The preprocessing details are presented in [supplementary material S3](#).

Network Construction

The adopted paradigm (detailed information is presented in [supplementary material S3](#)) consists of two types of conditions that differed in terms of WM load (0-back and 2-back). As the 0-back is not considered to be a WM task, we used it to help subjects familiarize themselves with the task procedure. Therefore, in the construction process of a functional connection matrix, we only concatenated the fMRI volumes obtained during the 4 blocks of 2-back performance.³¹ The mean time series was extracted from each of the 264 nodes using 6-mm spheres defined by the Power atlas.³⁷ A 264×264 symmetric matrix was generated for each participant by computing the Pearson correlation coefficients between the time series for each pair of ROIs. The resultant matrix was converted to normally distributed scores by using the Fisher's *z* transformation,

and the variance due to the linear effects of age, gender, and education years was removed to derive the corrected symmetric matrix.

Network measures at each density (sparsity) were calculated on the 264×264 weighted adjacency matrices, which were acquired by thresholding the symmetric matrices at a series of network densities, ranging from top 10% to 50% of all connections, with 2% increments, in line with a prior study.³⁸ The reason for choosing this range density is that network measures are less prone to nonbiological artifacts and noise in this density range.³⁹ Negative correlations were set to zero, in line with other studies of functional connectome construction.^{40,41} We did not use binarized matrices as binarization is arbitrary and can result in the loss of important illness-related biological features that can be captured by weighted network approaches.^{34,35} We used the Brain Connectivity Toolbox⁴² to quantify network measures and the Graph Analysis Toolbox⁴³ to compare the functional networks of patients and HCs.

Network Properties

We calculated sigma (small-worldness) and degree centrality on weighted, undirected networks. As sigma is a ratio of gamma (normalized clustering coefficient) to lambda (normalized characterized path length) (ie, $\sigma = \frac{\gamma}{\lambda}$), we also report gamma and lambda values. These normalized topological properties must be benchmarked against corresponding mean values of null random graphs (ie, $\gamma = \frac{C}{C_{null}}$ and $\lambda = \frac{L}{L_{null}}$, where C indicates the clustering coefficient, and L indicates the path length). We generated 20 null random networks^{44,45} with the same number of nodes, degree, and degree distribution as the network of interest. We further compared the clustering coefficient (strongly associated with gamma) of each node to obtain the regional alteration of the WM-related brain networks of patients with schizophrenia compared with that of HCs. We plotted the cumulative degree distribution curve of each group and defined nodes with greater than one standard deviation from the mean of all nodal mean degree values as “hubs” to identify the core component in facilitating intercommunication during the WM task. Previous studies have reported that brain functional networks display an exponentially truncated power-law distribution of nodal degree,^{46,47} that confers critical scale-free properties to the connectome. In line with the prior work on functional topology in schizophrenia,^{46,48} we did not expect this fundamental property to be altered in schizophrenia.

As influenced by the long-standing hypotheses of function segregation, an increasing body of studies concerning mental illness and cognition paid more attention to some particular subnetworks related to cognition,⁴⁹ but not the whole brain. In parallel with these studies, we parcellated the whole brain into subnetworks based

on Power atlas, isolated brain nodes of each subnetwork, and analyzed their topological characteristics (the details were given in the [supplementary material S5](#)).

Statistical Analysis

Group-related differences in demographic, clinical characteristics, and WM task performances were analyzed using a one-way analysis of variance and chi-square (χ^2) tests. Additionally, we conducted a nonparametric permutation test with 1000 repetitions to test the statistical significance of group-related differences in network properties across densities (more information in [supplementary material S6](#)). Furthermore, statistical maps of regional properties were generated after multiple comparison analysis (FDR corrected using the Benjamini-Hochberg method with $P < .05$). It is worth noting that dataset 2 was used only for validation; therefore, the correction for multiple comparisons was not applied for dataset 2. Importantly, all of the above analyses were conducted in dataset 1 and dataset 2 separately.

Exploratory Analysis

Moderation Analysis. We conducted a linear regression analysis to test the association of clinical symptoms, WM performance, and network properties. In this linear regression model, we defined the accuracy of 2-back as the dependent variable, clinical symptoms including SANS and SAPS as the predictor, global properties as the moderator variable, and scanning site as the control variables. We repeated the aforementioned moderation analysis in the 0-back condition and conducted a linear regression analysis for testing the association of sigma (under 2-back), medication dose, and WM accuracy.

Machine Learning. We employed global, subnetwork-level, and nodal topological properties for the subsequent pattern recognition using SVM toolkit LIBSVM (<http://www.csie.ntu.edu.tw/~cjlin/libsvm/>). The kernel function of SVM was set as the polynomial type, and other all related parameters were set as default. The general performance of the classifier was evaluated using two approaches. One approach used a 5-fold cross-validation after pooling dataset 1 and dataset 2; the second approach employed dataset 1 for classifier training and dataset 2 as the testing sample. Evaluation indices were calculated to assess classifier performance. Details of our machine-learning analysis are presented in [supplementary material S7](#).

Results

Participant Characteristics

The demographic and clinical variables are presented in [table 1](#). In dataset 1, we observed group-related differences with respect to gender ($P = .025$, $\chi^2 = 5.0$) and

Table 1. Demographic and Clinical Characteristics of Patients With Schizophrenia and HCs

	Dataset 1				Dataset 2			
	Patients (<i>n</i> = 155)	HCs (<i>n</i> = 96)	<i>P</i>	<i>T/χ</i> ²	Patients (<i>n</i> = 81)	HCs (<i>n</i> = 54)	<i>P</i>	<i>T/χ</i> ²
Age (y)	24.06 ± 5.6	23.96 ± 4.2	.13	1.53	18.08 ± 3.3	23.13 ± 3.7	<.001*	-7.36
Sex(M/F)	84/49	38/42	.025*	5.0	33/29	25/20	0.81	0.057
Education (y)	11.78 ± 2.6	14.2 ± 2.1	<.001*	-7.1	10.95 ± 2.6	13.79 ± 3.8	<.001*	-4.58
SAPS	21.14 ± 15.9	N/A	N/A	N/A	26.58 ± 20.6	N/A	N/A	N/A
SANS	34.4 ± 27.2	N/A	N/A	N/A	44.38 ± 40.3	N/A	N/A	N/A
Total dosage (mg/d)	8.7 ± 4.6	N/A	N/A	N/A	13 ± 8	N/A	N/A	N/A
Illness duration (M)	23.3 ± 29.2	N/A	N/A	N/A	24 ± 25.7	N/A	N/A	N/A
Treat_duration (M)	4.62 ± 9.7	N/A	N/A	N/A	11.6 ± 15.9	N/A	N/A	N/A
WAIS_information	16 ± 5.2	20.8 ± 4.7	<.001*	-6.7	15.8 ± 5.9	18.7 ± 5.4	.002*	-3.2
WAIS_digit_Sym	63.8 ± 15.6	88.8 ± 13.7	<.001*	-11	60.2 ± 17.8	89 ± 17	<.001*	-9
ACC_of_2-back (%)	69 ± 18	83 ± 13	<.001*	-5.6	66 ± 23	84 ± 14	<.001*	-4.82
ACC_of_0-back (%)	79 ± 26	93 ± 14	<.001*	-4.6	85 ± 22	93 ± 13	.023	-2.6

Note. *n*, number; SAPS, Scale for the Assessment of Positive Symptoms; SANS, Scale for the Assessment of Negative Symptoms; Treat_duration, Treatment duration; ACC_of_2Back, Accuracy under the 2-back condition; WAIS_information, information subscale of Wechsler Adult Intelligence Scale-Chinese Revised; WAIS_digit_Sym, digit symbol subscale of Wechsler Adult Intelligence Scale-Chinese Revised; ACC_of_0Back, Accuracy under the 0-back condition; N/A, not available; antipsychotic dosage refers to the dose equivalents for Olanzapine.⁷⁰

**P* value was calculated by independent two-sample *t*-test.

years of education ($P < .001$, $t = -7.1$). In dataset 2, we observed group-related differences in terms of age ($P < .001$, $t = -7.4$) and years of education ($P < .001$, $t = -4.58$). In both datasets 1 and 2, the performance of the patient group was worse than that of the HCs under 2-back (dataset 1: $P < .001$, $t = -5.6$; dataset 2: $P < .001$, $t = -4.8$).

Network Properties

We observed that patients with schizophrenia showed consistent results of all calculated global properties of the whole brain under 2-back in both datasets, compared with HCs. As presented in [figure 1](#), patients showed increased sigma under 2-back in both datasets (dataset 1: patients mean(SD) = 31(2.8), HCs mean(SD) = 29.2(4), FDA permutation test $P < .001$; dataset 2: patients mean(SD) = 30.6(2.9), HCs mean(SD) = 28.4(3.6), FDA permutation test $P = .003$), increased gamma (dataset 1: patients mean(SD) = 33.8(3), HCs mean(SD) = 31.9(4.2), FDA permutation test $P < .001$; dataset 2: patients mean(SD) = 34.4(3.3), HCs mean(SD) = 32.1(3.8), FDA permutation test $P = .0015$), but the alteration of lambda was not observed (dataset 1: patients mean(SD) = 22.6(0.5), HCs mean(SD) = 22.8(0.6), FDA permutation test $P = .064$; dataset 2: patients mean(SD) = 23.3(0.7), HCs mean(SD) = 23.5(0.7), FDA permutation test $P = .259$), compared with HCs. To ensure that our choice of the atlas did not bias findings, analyses of global properties were recomputed with AAL atlas, and consistent findings were observed (more details in [supplementary material S8](#) and [supplementary figure S2](#)). No significant differences were observed when

the sigma of the female patients was directly compared with male patients (See [supplementary material S9](#)). Furthermore, the examination of 0-back control condition revealed that topological changes attributable to simple attention and motor function during the WM task are relatively small (more information in [supplementary material S10](#) and [supplementary tables S1 and S2](#)).

Given the illness-specific changes in global clustering (gamma), we investigated the regional clustering coefficients and observed that in patients with schizophrenia nodes with higher clustering coefficient were distributed on the FPN and cingulo-opercular network (see [figure 2](#) and [table 2](#)). The results of dataset 2 are presented in [supplementary table S3](#). In the comparison of global properties on each isolated subnetwork, we did not observe any significant alteration of global properties of all subnetworks in patients with schizophrenia (see [supplementary figure S1](#)).

In accordance with previous studies,⁴⁶ we found the degree distribution of brain functional networks that generated in the current study followed an exponentially truncated power-law distribution (see [supplementary figure S4](#)). The degree distribution of patients with schizophrenia showed a shift to a more homogeneous form compared to HCs, with a reduction in the probability of finding high-degree as well as very low-degree nodes (see [figure 3](#)). There were significant differences between groups in terms of mean degree distribution parameters across densities: rank-ordering patients with schizophrenia > HCs for the power-law exponent, α (patients mean(SD) = 0.3(0.37); HCs mean(SD) = 0.15(0.37) two-sample *t*-test $P = .005$, $t = 2.9$), but rank-ordering HCs > patients with schizophrenia for the

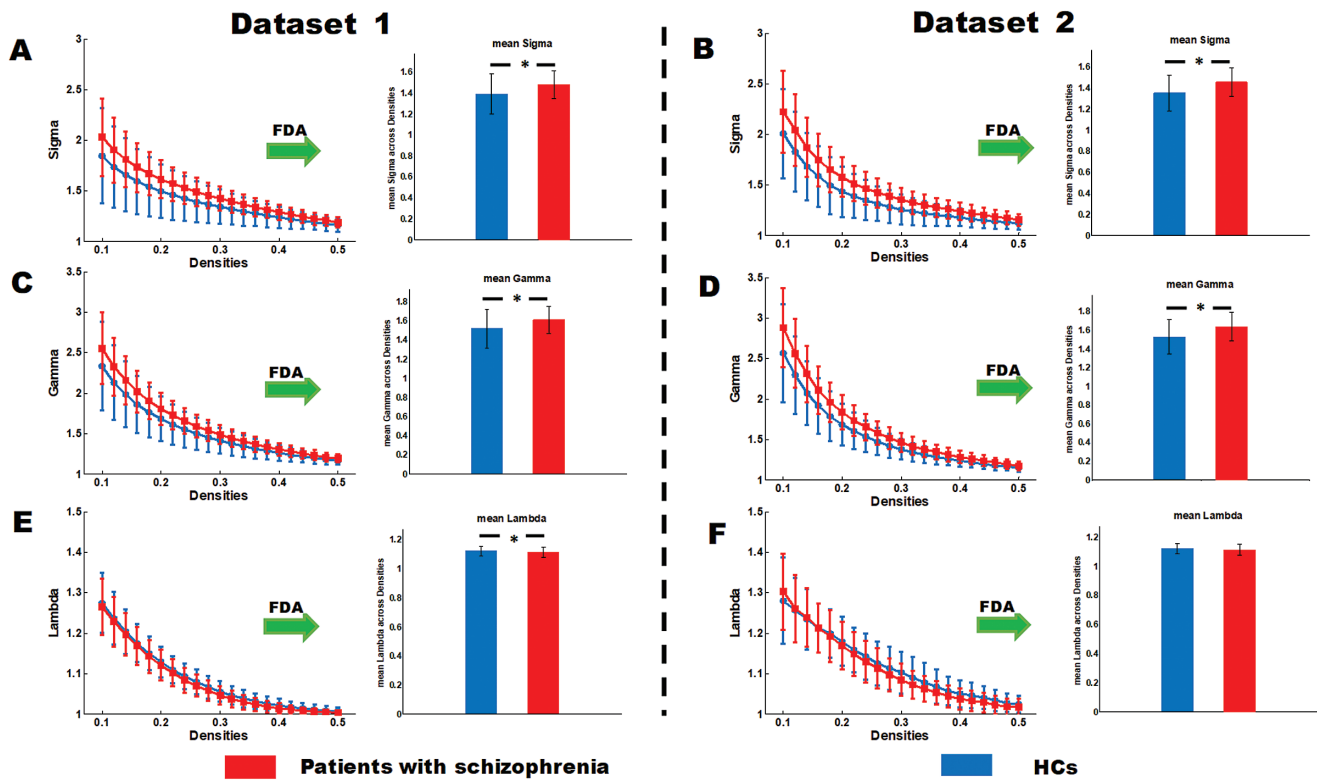


Fig. 1. Global properties of the whole-brain functional connectome calculated on Power atlas of patients with schizophrenia compared to that of HCs. The range of densities is 0.1: 0.02: 0.5, and symbol “*” represents $P < .05$. (A) Comparison of mean sigma across densities between two groups in dataset 1; (B) comparison of mean sigma across densities between two groups in dataset 2; (C) comparison of mean gamma across densities between two groups in dataset 2; (D) comparison of mean gamma across densities between two groups in dataset 2; (E) comparison of mean lambda across densities between two groups in dataset 1; (F) comparison of mean lambda across densities between two groups in dataset 2.

exponential cutoff, β (patients mean(SD) = 17.4(25.8); HCs mean(SD) = 33.1(29.2); two-sample t -test $P < .001$, $t = -3.9$). The number of hubs (ie, nodes > 1 SD of overall degree³⁸) was 54 in the HCs and 47 in patients with no obvious discrepancies in the location of the hub regions in the two groups (see [figure 3](#) and [supplementary table S4](#)). Notably, these findings were consistent with dataset 2 (see [supplementary figure S5](#) and [supplementary table S5](#)).

Exploratory Analysis

Moderation Analysis. We further assessed whether the altered sigma and gamma can moderate the impact of clinical symptoms on WM performance. As shown in [figure 4](#), sigma moderated the relationship between SANS and WM performance ($\beta = 0.2$, $P = .027$, $t = 2.236$). The detailed information of the moderation analysis was presented in [supplementary tables S6 and S7](#). There was no moderating effect for sigma on the relationship between SAPS and WM performance and for gamma on the relationship between clinical symptoms and WM performance. There were no moderating effects for sigma on the relationship between medication dose and WM performance. The sigma from 0-back task had no moderating effect on the relationship between clinical

symptoms and WM performance (see [supplementary figures S3 and S6](#)).

Machine Learning. From the two approaches used for evaluating the discriminating performance of the topological properties of the brain network, we achieved classification results with average accuracy, AUC, true-positive rate for schizophrenia, true-positive rate for HCs, of 71.4%, 0.69, 85.7%, and 52.8%, respectively. The evaluation parameters of those two validation approaches are presented in [supplementary table S8](#) and their receiver-operator characteristics plotted in [figure 4](#).

Discussion

To our knowledge, this is the first study to demonstrate consistent and generalizable changes in small-world global topology during WM performance across 2 datasets in schizophrenia. We report 3 key observations. Firstly, there is a significant increase in local clustering (especially in the FPN network), without notable changes in global integration in the whole-brain functional connectome during a WM task in schizophrenia. This resulted in an overall increase in small-worldness among patients. Secondly, there is a shift in the degree distribution to a more homogeneous form

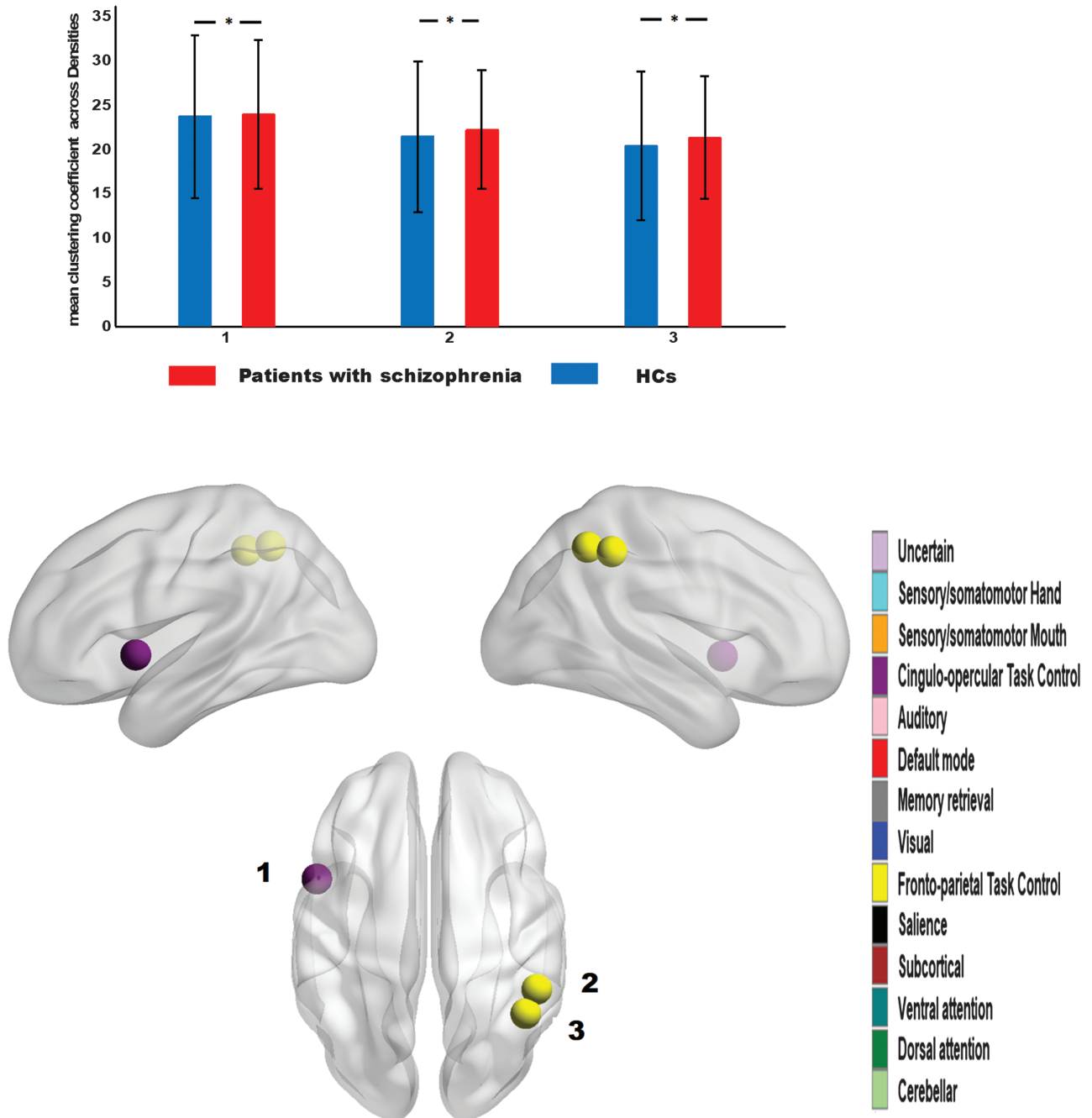


Fig. 2. Nodes showing significantly altered clustering coefficient in patients with schizophrenia compared to HCs. (A) The bar plots of the nodes with significantly altered clustering coefficient; (B) the spatial distribution of nodes with significantly altered clustering coefficient in patients.

(fewer hubs but more non-hubs) in patients with schizophrenia. Thirdly, in the presence of more severe negative symptom burden, an increase in small-worldness was associated with better WM accuracy though not reaching the performance of healthy controls. Thus, the context (task)-dependent modulation of the functional connectome appears to be inefficient to improve performance above par in a subgroup of patients with schizophrenia. The results from SVM analysis also indicate that the interplay between various levels of topological

parameters carries sufficient illness-specific information relevant to schizophrenia.

Increase in small-worldness is not associated with a concomitant increase in accuracy among patients and controls in our sample, in contrast to the performance advantage reported elsewhere in healthy controls.^{26,50} One reason for this might be the nature of topological change seen in schizophrenia; the small-world index is higher in patients due to an increased segregation, with no concomitant increase in integration. Interestingly, among healthy adults, increased

Table 2. Nodes Showing Significantly Altered Clustering Coefficient in Patients With Schizophrenia Compared to HCs in Dataset 1

Index	Coordinate (MNI)	Subsystem	Patients Mean(SD)	HCs Mean(SD)	FDR Corrected (<i>P</i> value)
Patients with schizophrenia > HCs					
1	[-51, 8, -2]	Cingulo-opercular	24(8.4)	23.7(9.2)	<.001
2	[49, -42, 45]	Frontoparietal	22.2(6.7)	21.4(8.5)	<.001
3	[44, -53, 47]	Frontoparietal	21.3(6.9)	20.3(8.4)	<.001
Patients with schizophrenia < HCs					
None					

Note. *P* value was calculated by FDA permutation test.

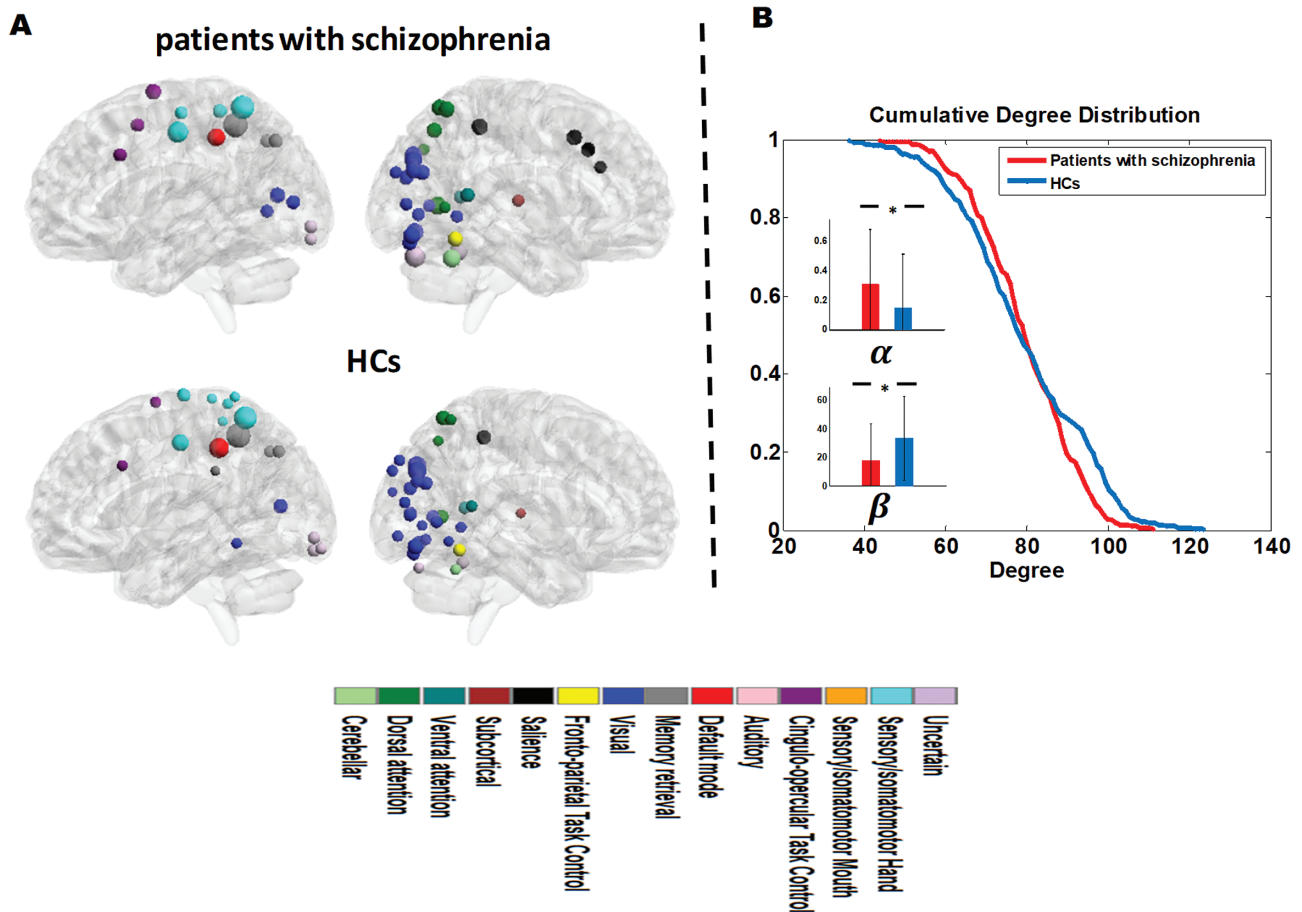


Fig. 3. Hubs of the whole-brain functional connectome in patients with schizophrenia and HCs. (A) The spatial distribution of hubs in patients with schizophrenia and HCs; (B) the cumulative degree distribution in patients with schizophrenia and HCs. (Inset) boxplots represent the within-group distributions and between-group differences in the two parameters: α (the power-law exponent) and β (the exponential cutoff); Symbol “*” indicates significant between-group differences.

segregation appears critical for motor execution, whereas distal integration is critical for working memory.⁵⁰ It is important to note that ketamine infusion, which provides a pharmacological model of acute psychosis, selectively reduces distal connectivity⁵¹⁻⁵³ but increases global⁵⁴ and short-distance regional connectivity⁵⁵ in humans and non-human primates. In terms of network topology, this translates to less-integrated and more-segregated functional connectome,^{56,57} an effect similar to our own observations in schizophrenia. Insofar as invoked changes in functional

connectivity relate to network plasticity,^{58,59} we speculate that the observed pattern in patients may indicate a tilt toward preferential proximal plasticity, as opposed to distal integrative plasticity, that may be linked to NMDA-related synaptic inefficiency. This pattern of segregation may aid in improving task performance to some extent (eg, by optimizing specific modules such as the motor system), especially when the demand is low, but not sustainable (or produce functional interference) at higher loads, probably contributing to the leftward shift of the typical inverted-U

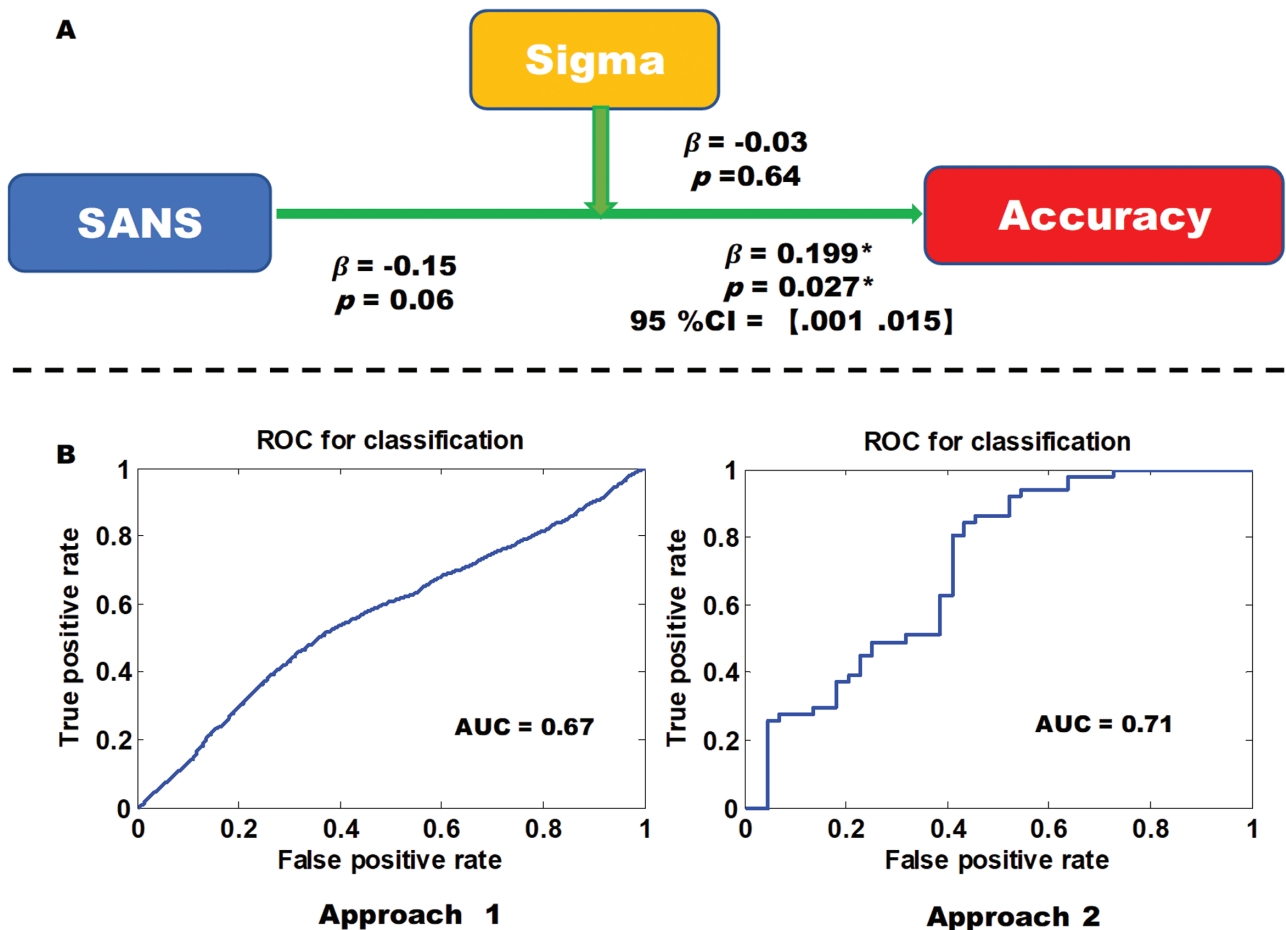


Fig. 4. Exploratory analysis results. (A) The moderating model of sigma on the relation of symptoms and WM performance; (B) The receiver-operating characteristics of the machine-learning analysis.

shaped trend in WM-related neural recruitment⁶⁰ in patients with schizophrenia.^{61,62}

We noted a notable shuffle in the degree distribution curve, with patients having significantly reduced high-degree hubs as well as low-degree nodes, indicating a degree of “liberalization” of degree centrality. This is consistent with the observation of hub de-escalation and redistribution during *n*-back task made in the study of Palaniyappan and Liddle et al,¹⁹ the observation of homogenization of degree during resting state made in the study of and Lo et al, and the observation of less fat-tailed degree distribution during the odd-ball task made in the study of Ma et al.^{46,63} Such an effect is likely in the context of widespread dendritic reduction (or pruning), wherein cortical hubs with highest number of functional synaptic connections get preferentially de-escalated, whereas the peripheral hubs increasingly come “on-line” when task demands arise.⁶⁴ Longitudinal neuroimaging studies are required to determine the relationship between structural brain changes and hub redistribution in schizophrenia.

Contrary to our initial expectation, we noted no significant relationship between WM accuracy and the burden of negative symptoms. In part, this may be due to the

pervasive selection bias in case-control studies of schizophrenia, wherein patients with low motivation, anhedonia, and apathy often do not participate in study recruitment, resulting in insufficient variance in negative symptom severity to make meaningful related observations. Nevertheless, we noted that in the presence of higher degree of negative symptoms, increased small-worldness (though not increased segregation per se) facilitated WM performance, albeit not reaching the level seen in healthy controls. If sigma can be taken as a physiological index of effort needed to achieve the desired WM accuracy, our mediation results indicate that in the presence of higher levels of negative symptoms, much higher physiological efforts are needed to reach even a modestly higher WM accuracy, but the accuracy level thus achieved is still considerably lower than what HCs achieve with less effort. Such inefficient compensation did not occur in relation to positive symptom burden, underscoring the link between the pathophysiology of WM deficits and negative symptoms in schizophrenia.

Our study had a number of strengths, including the use of two independent samples of patients performing the same task, a fairly large sample, the use of state-of-art graph-theoretical methods, and cross-validation

approaches to demonstrate reproducibility. Nevertheless, it is important to note that the results pertaining to regional nodal properties were somewhat different between the 2 datasets. While this may be due to a type 2 error in dataset 2 (as the sample size was ~50% less than dataset 1), it is also worth noting that dataset 2 comprised of subjects with adolescent-onset schizophrenia. Notwithstanding this, the observed consistency of aberrant task-related small-worldness and degree distribution supports the claim that these changes are a cardinal feature of the pathophysiology of schizophrenia, irrespective of the age of illness onset. Further, we used a limited *n*-back paradigm that precluded examination of the parametric effect of WM load. Load-sensitive WM tasks that provide meaningful measures in patients with schizophrenia are required to confirm our interpretations. All patients with schizophrenia were on antipsychotics. Medication administration may influence our findings, but the fact that our findings were replicated across 2 samples with different duration of medication exposure suggests that our observations are likely to withstand the confounding effects of antipsychotics.

Treatment strategies to alleviate WM deficits in schizophrenia are of great interest, though to date, empirical studies have shown mixed results.⁶⁵ Lack of understanding of the neural basis of WM performance in schizophrenia remains as a critical gap in the development of novel disease-modifying, pro-cognitive intervention.^{66,67} Furthermore, animal models of cognitive impairment are of limited utility to study the subtle aspects of cognition that are unique to humans, with many putative procognitive interventions in animal studies failing to show comparable effects in humans.^{68,69} Utilizing a reliable human neuroimaging methodology could allow us to test the efficacy of putative interventions in humans at an early stage, thus providing an efficient filtering for agents to undergo later phase studies. By demonstrating a mechanistic link between inefficient functional segregation (clustering), hub redistribution, and impaired *n*-back performance in schizophrenia, our study raises the possibility of an fMRI-based “engagement” target for developing novel WM-enhancing interventions (we also expanded this point in [supplementary material S11](#)). It also raises the question of whether treatments that increase distal integrative connectivity, rather than proximal clustering, are likely to be promising precognitive agents in schizophrenia.

Supplementary Material

Supplementary data are available at *Schizophrenia Bulletin* online.

Funding

This work was supported by the China Precision Medicine Initiative (2016YFC0906300 to ZL), the National

Natural Science Foundation of China (81561168021 to ZL, 81701325 to GW), the China Postdoctoral Science Foundation (2018M643007 to JY), and the Postdoctoral Research Fund of Xiangya No.2 Hospital, Central South University (207161 to JY). This work was partly supported by Canadian Institutes of Health Research Foundation Grant (375104/2017), AMOSO Opportunities fund, Bucke Family Fund, and Kilborn Fund for Internalisation from Western University to L.P. L.P. also acknowledges support from the Tanna Schulich Endowment Chair.

Acknowledgments

L.P. reports personal fees from Otsuka Canada, SPMM Course Limited, UK, Canadian Psychiatric Association; book royalties from Oxford University Press; investigator-initiated educational grants from Janssen Canada, Sunovion, and Otsuka Canada outside the submitted work. All other authors report no relevant conflicts.

References

- Lewis DA. Cortical circuit dysfunction and cognitive deficits in schizophrenia – implications for preemptive interventions. *Eur J Neurosci*. 2012;35(12):1871–1878.
- McGurk SR, Coleman T, Harvey PD, et al. The relationship of working memory and executive dysfunction in poor outcome schizophrenia. *Biol Psychiat*. 2001;49(8):56s–57s.
- Green MF, Nuechterlein KH. Should schizophrenia be treated as a neurocognitive disorder? *Schizophr Bull*. 1999;25(2):309–319.
- Park S, Püschel J, Sauter BH, Rentsch M, Hell D. Spatial working memory deficits and clinical symptoms in schizophrenia: a 4-month follow-up study. *Biol Psychiatry*. 1999;46(3):392–400.
- Hui C, Li YK, Li AWY, et al. Visual working memory deterioration preceding relapse in psychosis. *Early Interv Psychia*. 2016;10:165–165.
- Pantelis C, Stuart GW, Nelson HE, Robbins TW, Barnes TR. Spatial working memory deficits in schizophrenia: relationship with tardive dyskinesia and negative symptoms. *Am J Psychiatry*. 2001;158(8):1276–1285.
- Cameron Carter LR, Nordahl T, Chaderjian M, Kraft L, O’Shora-Celaya L. Spatial working memory deficits and their relationship to negative symptoms in unmedicated schizophrenia patients. *Biol Psychiat*. 1996;40(9).
- González-Ortega I, de Los Mozos V, Echeburúa E, et al. Working memory as a predictor of negative symptoms and functional outcome in first episode psychosis. *Psychiatry Res*. 2013;206(1):8–16.
- Nejad AB, Madsen KH, Ebdrup BH, et al. Neural markers of negative symptom outcomes in distributed working memory brain activity of antipsychotic-naïve schizophrenia patients. *Int J Neuropsychopharmacol*. 2013;16(6):1195–1204.
- Carlsson R, Nyman H, Ganse G, Cullberg J. Neuropsychological functions predict 1- and 3-year outcome in first-episode psychosis. *Acta Psychiatr Scand*. 2006;113(2):102–111.

11. Ventura J, Helleman GS, Thames AD, Koellner V, Nuechterlein KH. Symptoms as mediators of the relationship between neurocognition and functional outcome in schizophrenia: a meta-analysis. *Schizophr Res*. 2009;113(2–3):189–199.
12. Thomas ML, Green MF, Helleman G, et al. Modeling deficits from early auditory information processing to psychosocial functioning in schizophrenia. *JAMA Psychiatry*. 2017;74(1):37–46.
13. Pomarol-Clotet E, Salvador R, Sarró S, et al. Failure to deactivate in the prefrontal cortex in schizophrenia: dysfunction of the default mode network? *Psychol Med*. 2008;38(8):1185–1193.
14. Whitfield-Gabrieli S, Thermenos HW, Milanovic S, et al. Hyperactivity and hyperconnectivity of the default network in schizophrenia and in first-degree relatives of persons with schizophrenia. *Proc Natl Acad Sci U S A*. 2009;106(4):1279–1284.
15. Godwin D, Ji A, Kandala S, Mamah D. Functional connectivity of cognitive brain networks in schizophrenia during a working memory task. *Front Psychiatry*. 2017;8.
16. Pu W LQ, Palaniyappan L, Xue Z, Yao S, Feng J, Liu Z. Failed cooperative, but not competitive, interaction between large-scale brain networks impairs working memory in schizophrenia. *Psychol Medicine* 2016;46(6).
17. Zhou Y, Zeidman P, Wu S, et al. Altered intrinsic and extrinsic connectivity in schizophrenia. *Neuroimage Clin*. 2018;17:704–716.
18. Repovs G, Barch DM. Working memory related brain network connectivity in individuals with schizophrenia and their siblings. *Front Hum Neurosci*. 2012;6.
19. Palaniyappan L, Liddle PF. Diagnostic discontinuity in psychosis: a combined study of cortical gyrification and functional connectivity. *Schizophr Bull*. 2014;40(3):675–684.
20. Meyer-Lindenberg A, Poline JB, Kohn PD, et al. Evidence for abnormal cortical functional connectivity during working memory in schizophrenia. *Am J Psychiatry*. 2001;158(11):1809–1817.
21. Ettinger U, Williams SC, Fannon D, et al. Functional magnetic resonance imaging of a parametric working memory task in schizophrenia: relationship with performance and effects of antipsychotic treatment. *Psychopharmacology (Berl)*. 2011;216(1):17–27.
22. Kim MA, Tura E, Potkin SG, et al.; FBIRN. Working memory circuitry in schizophrenia shows widespread cortical inefficiency and compensation. *Schizophr Res*. 2010;117(1):42–51.
23. Tononi G. A measure for brain complexity: relating functional segregation and integration in the nervous system. *Biol Psychiat*. 2002;51(8):151s–151s.
24. Bullmore E, Sporns O. Complex brain networks: graph theoretical analysis of structural and functional systems. *Nat Rev Neurosci*. 2009;10(3):186–198.
25. Stevens AA, Tappan SC, Garg A, Fair DA. Functional brain network modularity captures inter- and intra-individual variation in working memory capacity. *Plos One*. 2012;7(1).
26. Fornito A, Yoon J, Zalesky A, Bullmore ET, Carter CS. General and specific functional connectivity disturbances in first-episode schizophrenia during cognitive control performance. *Biol Psychiatry*. 2011;70(1):64–72.
27. Zhao Z, Cheng Y, Li Z, Yu Y. Altered small-world networks in first-episode schizophrenia patients during cool executive function task. *Behav Neurol*. 2018;2018:2191208.
28. Jhung K, Cho SH, Jang JH, et al. Small-world networks in individuals at ultra-high risk for psychosis and first-episode schizophrenia during a working memory task. *Neurosci Lett*. 2013;535:35–39.
29. Micheloyannis S, Pachou E, Stam CJ, et al. Small-world networks and disturbed functional connectivity in schizophrenia. *Schizophr Res*. 2006;87(1–3):60–66.
30. Kambeitz J, Kambeitz-Ilankovic L, Cabral C, et al. Aberrant functional whole-brain network architecture in patients with schizophrenia: a meta-analysis. *Schizophrenia Bull*. 2016;42:S13–S21.
31. He H, Sui J, Yu Q, et al. Altered small-world brain networks in schizophrenia patients during working memory performance. *PLoS One*. 2012;7(6):e38195.
32. He H, Sui J, Yu QB, et al. Altered small-world brain networks in schizophrenia patients during working memory performance. *Plos One*. 2012;7(6).
33. Siebenhüner F, Weiss SA, Coppola R, Weinberger DR, Bassett DS. Intra- and inter-frequency brain network structure in health and schizophrenia. *Plos One*. 2013;8(8).
34. van den Heuvel MP, de Lange SC, Zalesky A, Seguin C, Yeo BTT, Schmidt R. Proportional thresholding in resting-state fMRI functional connectivity networks and consequences for patient-control connectome studies: issues and recommendations. *Neuroimage*. 2017;152:437–449.
35. Váša F, Bullmore ET, Patel AX. Probabilistic thresholding of functional connectomes: application to schizophrenia. *Neuroimage*. 2018;172:326–340.
36. Walter M, Alizadeh S, Jamalabadi H, et al. Translational machine learning for psychiatric neuroimaging. *Prog Neuropsychopharmacol Biol Psychiatry*. 2019;91:113–121.
37. Power JD, Cohen AL, Nelson SM, et al. Functional network organization of the human brain. *Neuron*. 2011;72(4):665–678.
38. Singh MK, Kesler SR, Hadi Hosseini SM, et al. Anomalous gray matter structural networks in major depressive disorder. *Biol Psychiatry*. 2013;74(10):777–785.
39. Kaiser M, Hilgetag CC. Nonoptimal component placement, but short processing paths, due to long-distance projections in neural systems. *Plos Comput Biol*. 2006;2(7):805–815.
40. Rubinov M, Sporns O. Complex network measures of brain connectivity: uses and interpretations. *Neuroimage*. 2010;52(3):1059–1069.
41. Rubinov M, Sporns O. Weight-conserving characterization of complex functional brain networks. *Neuroimage*. 2011;56(4):2068–2079.
42. M Rubinov RK, Hagmann P, Sporns O. Brain connectivity toolbox: a collection of complex network measurements and brain connectivity datasets. *Neuroimaging*. 2009;47(S1).
43. Hosseini SM, Hoefl F, Kesler SR. GAT: a graph-theoretical analysis toolbox for analyzing between-group differences in large-scale structural and functional brain networks. *PLoS One*. 2012;7(7):e40709.
44. Palaniyappan L, Park B, Balain V, Dangi R, Liddle P. Abnormalities in structural covariance of cortical gyrification in schizophrenia. *Brain Struct Funct*. 2015;220(4):2059–2071.
45. Das T, Borgwardt S, Hauke DJ, et al. Disorganized gyrification network properties during the transition to psychosis. *JAMA Psychiatry*. 2018;75(6):613–622.
46. Lo CY, Su TW, Huang CC, et al. Randomization and resilience of brain functional networks as systems-level endophenotypes of schizophrenia. *Proc Natl Acad Sci U S A*. 2015;112(29):9123–9128.
47. Achard S, Salvador R, Whitcher B, Suckling J, Bullmore E. A resilient, low-frequency, small-world human brain functional

- network with highly connected association cortical hubs. *J Neurosci*. 2006;26(1):63–72.
48. Lynall ME, Bassett DS, Kerwin R, et al. Functional connectivity and brain networks in schizophrenia. *J Neurosci*. 2010;30(28):9477–9487.
 49. Sheffield JM, Kandala S, Tamminga CA, et al. Transdiagnostic associations between functional brain network integrity and cognition. *JAMA Psychiatry*. 2017;74(6):605–613.
 50. Cohen JR, D’Esposito M. The segregation and integration of distinct brain networks and their relationship to cognition. *J Neurosci*. 2016;36(48):12083–12094.
 51. Mueller F, Musso F, London M, de Boer P, Zacharias N, Winterer G. Pharmacological fMRI: effects of subanesthetic ketamine on resting-state functional connectivity in the default mode network, salience network, dorsal attention network and executive control network. *Neuroimage Clin*. 2018;19:745–757.
 52. Muthukumaraswamy SD, Shaw AD, Jackson LE, Hall J, Moran R, Saxena N. Evidence that subanesthetic doses of ketamine cause sustained disruptions of nmda and ampa-mediated frontoparietal connectivity in humans. *J Neurosci*. 2015;35(33):11694–11706.
 53. Joules R, Doyle OM, Schwarz AJ, et al. Ketamine induces a robust whole-brain connectivity pattern that can be differentially modulated by drugs of different mechanism and clinical profile. *Psychopharmacology (Berl)*. 2015;232(21–22):4205–4218.
 54. Driesen NR, McCarthy G, Bhagwagar Z, et al. Relationship of resting brain hyperconnectivity and schizophrenia-like symptoms produced by the NMDA receptor antagonist ketamine in humans. *Mol Psychiatry*. 2013;18(11):1199–1204.
 55. Rao JS, Liu Z, Zhao C, et al. Ketamine changes the local resting-state functional properties of anesthetized-monkey brain. *Magn Reson Imaging*. 2017;43:144–150.
 56. Becker R, Braun U, Schwarz AJ, et al. Species-conserved reconfigurations of brain network topology induced by ketamine. *Transl Psychiat*. 2016;6
 57. Lv Q, Yang L, Li G, et al. Large-Scale persistent network reconfiguration induced by ketamine in anesthetized monkeys: relevance to mood disorders. *Biol Psychiatry*. 2016;79(9):765–775.
 58. Tardif CL, Gauthier CJ, Steele CJ, et al. Advanced MRI techniques to improve our understanding of experience-induced neuroplasticity. *Neuroimage*. 2016;131:55–72.
 59. Kelly C, Castellanos FX. Strengthening connections: functional connectivity and brain plasticity. *Neuropsychol Rev*. 2014;24(1):63–76.
 60. Kirschen MP, Chen SH, Schraedley-Desmond P, Desmond JE. Load- and practice-dependent increases in cerebro-cerebellar activation in verbal working memory: an fMRI study. *Neuroimage*. 2005;24(2):462–472.
 61. Manoach DS. Prefrontal cortex dysfunction during working memory performance in schizophrenia: reconciling discrepant findings. *Schizophr Res*. 2003;60(2–3):285–298.
 62. Callicott JH, Mattay VS, Verchinski BA, Marenco S, Egan MF, Weinberger DR. Complexity of prefrontal cortical dysfunction in schizophrenia: more than up or down. *Am J Psychiatry*. 2003;160(12):2209–2215.
 63. Ma S, Calhoun VD, Eichele T, Du W, Adalı T. Modulations of functional connectivity in the healthy and schizophrenia groups during task and rest. *Neuroimage*. 2012;62(3):1694–1704.
 64. Palaniyappan L. Inefficient neural system stabilization: a theory of spontaneous resolutions and recurrent relapses in psychosis. *J Psychiatry Neurosci*. 2019;44(5):1–17.
 65. Lett TA, Voineskos AN, Kennedy JL, Levine B, Daskalakis ZJ. Treating working memory deficits in schizophrenia: a review of the neurobiology. *Biol Psychiatry*. 2014;75(5):361–370.
 66. Dolan RJ. Neuroimaging of cognition: past, present, and future. *Neuron*. 2008;60(3):496–502.
 67. Woo CW, Chang LJ, Lindquist MA, Wager TD. Building better biomarkers: brain models in translational neuroimaging. *Nat Neurosci*. 2017;20(3):365–377.
 68. Winship IR, Dursun SM, Baker GB, et al. An overview of animal models related to schizophrenia. *Can J Psychiatry*. 2019;64(1):5–17.
 69. Young JW, Geyer MA. Developing treatments for cognitive deficits in schizophrenia: the challenge of translation. *J Psychopharmacol*. 2015;29(2):178–196.
 70. Leucht S, Samara M, Heres S, et al. Dose equivalents for second-generation antipsychotic drugs: the classical mean dose method. *Schizophr Bull*. 2015;41(6):1397–1402.